

# Blowup dynamics of coherently driven polariton condensates

S. S. Gavrilov

*Institute of Solid State Physics, RAS, Chernogolovka, 142432, Russia*

(Dated: June 9, 2018)

Basing on the Gross-Pitaevskii equations, it is predicted that a repulsive (defocusing) interaction makes a 2D polariton condensate able to accumulate its energy under above-resonance optical pumping. The energy can be accumulated during a lot of polariton lifetimes, resulting in the state in which the mismatch of the pump frequency is compensated by the blueshift of the polariton resonance. The process begins when the field density reaches the parametric scattering threshold that is inversely proportional to the polariton lifetime. Although the increase in energy may be arbitrarily slow in its beginning, it is followed by a blowup. This scenario applies to the case of the transitions between steady states in multistable cavity-polariton systems. There is a tradeoff between the latency of the transitions and the pump power involving them.

PACS numbers: 71.36.+c, 42.65.Pc, 42.55.Sa

## I. INTRODUCTION

This study is devoted to the problem of non-equilibrium transitions in multistable cavity-polariton systems. Bi- and multistability of nonlinear media in which gain or decay rate ( $\gamma$ ) of light shows a threshold behavior had been studied for decades. Less known is another type of bistability that was predicted<sup>1</sup> to occur under resonant optical excitation of a macroscopically coherent state of bosons with a spin of 1 and a repulsive two-particle interaction, such as exciton gas in semiconductors. Due to the interaction the condensate level  $\hbar\omega_c$  shows a blueshift with increasing its population density  $n$ . If the frequency of the pump wave exceeds  $\omega_c$ , the positive feedback loop between  $n$  and  $\omega_c$  makes the system unstable within a finite interval of  $n$ . This kind of optical bistability, stemming from “intrinsic” interactions in a Bose gas rather than a non-linearity of a medium, has recently been observed in cavity-polariton systems.<sup>2–9</sup>

Cavity polaritons are composite bosons trapped in a cavity active layer due to the strong exciton-photon coupling.<sup>10–12</sup> Their lifetime is very small ( $\tau \sim 10^{-12} - 10^{-11}$  s in GaAs based microcavities); yet their interaction strength provides a blueshift that exceeds the resonance width ( $\hbar\gamma = \hbar/\tau$ ) even at comparatively low pump densities where the system can still be considered as a weakly non-ideal gas of bosons. The steady-state intensity of the driven mode can vary over more than an order of magnitude near critical (threshold) values of the pump density.<sup>5,6</sup> Polariton multistability allows switching the cavity between distinct steady states those, in a general case, differ in both intensity and polarization.<sup>8,13–15</sup> Recently there have been reported the transitions between linear and circular as well as right- and left-circular polarization states, which proceed on the scale of picoseconds under a constantly polarized pump wave.<sup>16–18</sup> The minimum switching time is comparable to  $\tau$ <sup>19</sup> and the minimum size of a “multistable cell” is several microns.<sup>5</sup> In its turn, the multistability gives rise to a spectacular row of collective phenomena in polariton physics, such as self-organized optical parametric oscillation (OPO),<sup>20,21</sup> spin rings,<sup>6,7,14</sup> threshold-like screening of surface acoustic waves,<sup>22</sup> and bright polariton solitons.<sup>23–25</sup> The combination of all-optical tunability, compactness and a high speed of transitions makes cavity-polariton systems in-

teresting for applications in the field of digital processing.

In this work we explore the dynamics of the bistability-initiated transitions. Using the Gross-Pitaevskii equations, we have found that a passage from the low- to high-energy state is mediated by the parametric scattering into signal/idler modes whose in-plane wave vectors differ from that of the pumped mode. Such scattering, which also shows a threshold onset with increasing pump power and is known to result in OPO states under pumping near the “magic angle”,<sup>26–30</sup> was not, however, taken into account in the studies of the multistability under normal-incidence pump.<sup>2,13–15</sup> Here we show that inter-mode scattering can have a drastic impact upon the multistability thresholds and duration of the transitions between steady states. The scattered modes (“signals”) are fed by the pumped mode that starts to break-up above the scattering threshold; importantly, this process is accompanied by a growth of both the “signal” and pumped mode amplitudes even at constant pump power. Although the growth can be arbitrarily slow in its beginning, with time it is followed by an explosive amplification of the pumped mode and a transition to the upper branch of stability. This effect is essentially collective; it cannot be reproduced within the framework of three-mode OPO models with fixed “signal” and “idler” wave vectors.

Similar scenarios, which imply a hyperbolic growth, or a singularity being reached in a finite time, are often referred to as regimes (or solutions) *with blowup*. Besides various models in many areas of knowledge, they are predicted to exist in systems described by the Schrödinger equation with cubic nonlinearity, also known as the Gross-Pitaevskii equation. If the system is conservative and the sign of the nonlinear term corresponds to *attractive* interaction, then singular solutions occur due to an intense self-focusing of the field.<sup>31,32</sup> By contrast, in this work we face a qualitatively new type of blowup behavior that takes place in systems described by the Gross-Pitaevskii equations with (i) a *repulsive* interaction and (ii) allowance made for both dissipation and coherent driving.

The paper is organized as follows. In Sec. II we analyze the effects of bistability and parametric scattering. The method is based on the Bogoliubov approximation and is widely used for studying OPO states in cavity-polariton systems.<sup>3,4,27,28,30,33–35</sup> Here our particular aim is to establish

the relation between the scattering and bistability thresholds for the case of pumping near normal incidence. In Sec. III we study the condensate above the scattering threshold and prove that no steady states can be formed below the catastrophe point in which intra-cavity field grows explosively; that is the central point of our work. Section IV, which can be read independently of Sec. III, contains a qualitative description and discussion of the main results. In Sec. V we give a numerical example that illustrates the considered evolution scenario. Finally, Sec. VI contains concluding remarks.

## II. BISTABILITY VS. PARAMETRIC SCATTERING: SETTING UP THE PROBLEM

The dispersion law for cavity polaritons has the form

$$\omega_{\text{LP,UP}}(\mathbf{k}) = \frac{1}{2}[\omega_C(\mathbf{k}) + \omega_X(\mathbf{k}) \pm \frac{1}{2}\sqrt{[\omega_C(\mathbf{k}) - \omega_X(\mathbf{k})]^2 + 4g^2}], \quad (1)$$

where  $\omega_{C,X}(\mathbf{k}) = \omega_{C,X}^{(0)} + \hbar\mathbf{k}^2/2m_{C,X}$  are the 2D cavity-photon (C) and exciton (X) frequencies,  $\mathbf{k}$  the in-plane wave vector,  $g$  the exciton-photon coupling constant; LP and UP stand for the lower and upper polariton branches. The photon mass  $m_C \sim 10^{-5}m_e$  is much smaller than the exciton mass  $m_X \sim 10^{-1}m_e$ ; therefore  $\omega_X$  can be considered constant at small  $k$ . In GaAs cavities  $\hbar g$  is of the order of several meV and largely exceeds the width of both photon and exciton levels ( $\hbar\gamma \sim 0.1$  meV). A plane wave with frequency  $\omega_p$  and incidence angle  $\theta$  excites polaritons with  $k_p = \omega_p \sin(\theta)/c$ . The presence of the upper dispersion branch will be further neglected on the assumption that  $|\omega_p - \omega_{\text{LP}}(k_p)| \ll \omega_{\text{UP}}(k_p) - \omega_{\text{LP}}(k_p)$ .

Throughout this work we assume that the state of the polariton system is macroscopically coherent under the conditions of coherent (plane-wave) pumping. Therefore its evolution is described by the Gross-Pitaevskii equation. In the  $k$ -space representation it reads<sup>3</sup>

$$i\frac{\partial}{\partial t}\psi(\mathbf{k},t) = [\omega(\mathbf{k}) - i\gamma(\mathbf{k})]\psi(\mathbf{k},t) + \delta(\mathbf{k},\mathbf{k}_p)f e^{-i\omega_p t} + V \sum_{\mathbf{q}_1,\mathbf{q}_2} \psi^*(\mathbf{q}_1 + \mathbf{q}_2 - \mathbf{k},t) \psi(\mathbf{q}_1,t) \psi(\mathbf{q}_2,t). \quad (2)$$

Here  $f$  is the pump amplitude,  $\psi$  the intra-cavity field (“macroscopic wavefunction”),  $\omega = \omega_{\text{LP}}$  the eigenfrequency and  $\gamma$  the decay rate;  $V > 0$  is the strength of the polariton-polariton interaction per unit area,  $\delta$  is Kronecker delta. Amplitudes  $f$  and  $\psi$  are expressed in arbitrary units, however,  $V|\psi|^2$  has the dimension of frequency and determines the resonance blueshift. The spin degrees of freedom are neglected, which corresponds to the case of pumping with circularly polarized light,<sup>13,15</sup> since the interaction between opposite-spin polaritons as well as TE/TM splitting can be considered negligible in isotropic cavities near  $k_p = 0$ .

Within the one-mode approximation, i.e.  $\psi(\mathbf{k},t) = \delta(\mathbf{k},\mathbf{k}_p)\psi_p e^{-i\omega_p t}$ , the response of the driven mode is defined

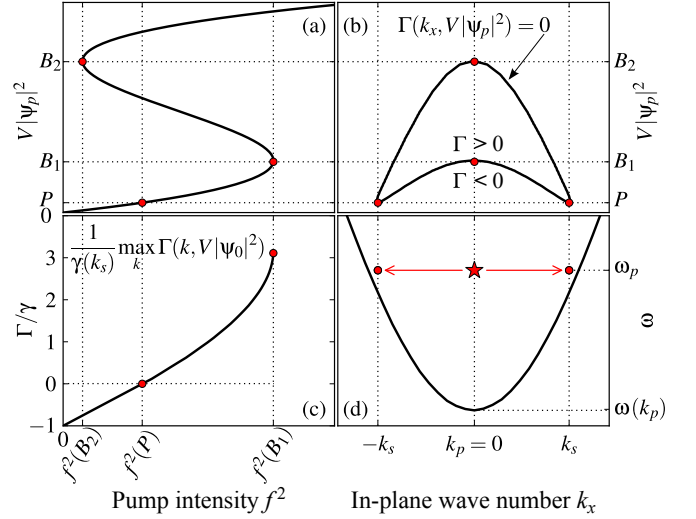


FIG. 1. (a) Intra-cavity field  $|\psi_p|^2$  as function of  $f^2$  in the one-mode approximation [see Eq. (3)]; (b) solutions (9) of equation  $\Gamma(k, V|\psi_p|^2) = 0$  defining the boundary between parametrically stable ( $\Gamma < 0$ ) and unstable ( $\Gamma > 0$ ) modes; (c) gain rate of scattered modes  $\max_k \Gamma(k, V|\psi_p|^2)/\gamma(k_s)$  at  $V|\psi_p|^2 < B_1$ , expressed in units of the polariton decay rate; (d) bare dispersion law and a scheme of parametric scattering. The solutions are obtained at  $\hbar[\omega_p - \omega(k_p)] = 0.5$  meV and  $\hbar\gamma \approx 0.04$  meV.

by the equation

$$|\psi_p|^2 = \frac{f^2}{[\omega_p - \omega(\mathbf{k}_p) - V|\psi_p|^2]^2 + [\gamma(\mathbf{k}_p)]^2}. \quad (3)$$

If  $\omega_p - \omega(\mathbf{k}_p) > \sqrt{3}\gamma(\mathbf{k}_p)$ , the dependence of  $|\psi_p|^2$  on  $f^2$  has the form of an S-shaped curve [Fig. 1(a)].<sup>1-3</sup> The solutions with negative derivative  $d(f^2)/d(|\psi_p|^2)$  are asymptotically unstable (see below). They lie within the interval  $B_1 < V|\psi_p|^2 < B_2$ , where

$$B_{1,2} = \frac{2}{3}[\omega_p - \omega(\mathbf{k}_p)] \pm \frac{1}{3}\sqrt{[\omega_p - \omega(\mathbf{k}_p)]^2 - 3[\gamma(\mathbf{k}_p)]^2}. \quad (4)$$

Attainment of  $V|\psi_p|^2 = B_1$  yields transition to the upper steady-state branch.

Besides the bistability effect, increasing density can involve loss of stability due to elastic two-particle scattering from  $\mathbf{k} = \mathbf{k}_p$  to the “signal” ( $\mathbf{k}_s, \tilde{\omega}_s$ ) and “idler” ( $\mathbf{k}_i, \tilde{\omega}_i$ ) modes.<sup>3,27,28</sup> According to the conservation laws,

$$2\mathbf{k}_p = \mathbf{k}_s + \mathbf{k}_i \quad \text{and} \quad 2\hbar\omega_p = \hbar\tilde{\omega}_s + \hbar\tilde{\omega}_i, \quad (5)$$

or

$$2\omega_p = \tilde{\omega}(\mathbf{k}) + \tilde{\omega}(2\mathbf{k}_p - \mathbf{k}), \quad (6)$$

where  $\tilde{\omega} = \tilde{\omega}(\mathbf{k})$  is a renormalized eigenfrequency. The scattering directions and threshold can be found using the Bogoliubov approximation, that is

$$\psi(\mathbf{k},t) = \delta(\mathbf{k},\mathbf{k}_p)\psi_p e^{-i\omega_p t} + \tilde{\psi}(\mathbf{k}) e^{-i\tilde{\omega}(\mathbf{k})t}, \quad (7)$$

$$|\tilde{\psi}(\mathbf{k})| \ll |\psi_p| \quad \text{for each } \mathbf{k}. \quad (8)$$

Under the above assumptions (6)–(8), the Gross-Pitaevskii equation (2) and its complex conjugate form a  $2 \times 2$  linear problem connecting  $\tilde{\psi}(\mathbf{k})$  and  $\tilde{\psi}^*(2\mathbf{k}_p - \mathbf{k})$ . Then solving the characteristic equation yields frequencies  $\Omega = \Omega(\mathbf{k}, V|\psi_p|^2)$  of above-condensate states. Stationary solutions  $\psi_p$  at which  $\Gamma = \text{Im}\Omega(\mathbf{k}, V|\psi_p|^2)$  takes positive values at any  $\mathbf{k}$  are asymptotically unstable. Equation  $\Gamma(\mathbf{k}, V|\psi_p|^2) = 0$  implicitly defines the scattering threshold  $V|\psi_p|^2 = P$  as function of the corresponding “signal” wave vector  $\mathbf{k}$ .

Figure 1(b) presents a typical solution of the equation  $\Gamma = 0$  at  $\mathbf{k}_p = 0$ ; Fig. 1(c) shows the largest (over  $\mathbf{k}$ ) gain rate  $\Gamma$  at  $V|\psi_p|^2 < B_1$ ; parametric scattering is schematically drawn in Fig. 1(d).

At  $\mathbf{k}_p = 0$  the scattering thresholds read

$$P_{1,2}(\mathbf{k}) = \frac{2}{3}[\omega_p - \omega(\mathbf{k})] \mp \frac{1}{3}\sqrt{[\omega_p - \omega(\mathbf{k})]^2 - 3[\gamma(\mathbf{k})]^2}; \quad (9)$$

these are the two nearly parabolic curves seen in Fig. 1(b). For simplicity, let  $\gamma(\mathbf{k})$  be constant. The scattering from  $\mathbf{k}_p = 0$  to  $\mathbf{k}_s \neq \mathbf{k}_p$  is impossible at  $\omega_p - \omega(\mathbf{k}_p) < \sqrt{3}\gamma$ , i. e. in the absence of bistability, because  $\omega(\mathbf{k}_s) > \omega(\mathbf{k}_p)$ . On the other hand,  $dP_1(\mathbf{k})/d[\omega_p - \omega(\mathbf{k})] > 0$  at  $\omega_p - \omega(\mathbf{k}) > 2\gamma$  and, hence,  $P_1(\mathbf{k}_s \neq \mathbf{k}_p) < B_1$ , i. e. the scattering threshold is at the lower branch of one-mode solutions. Then, with due regard for all scattering directions,

$$P = \min_{\mathbf{k}} P_1(\mathbf{k}) = \gamma \quad \text{if} \quad \omega_p - \omega(\mathbf{k}_p = 0) > 2\gamma; \quad (10)$$

the minimum is reached at  $\mathbf{k} = \mathbf{k}_s$  where  $\omega_p - \omega(\mathbf{k}_s) = 2\gamma$ . Finally, one can make certain that

$$f(B_2) < f(P) < f(B_1) \quad (11)$$

(see. Fig. 1), i. e.  $P$  is always within the bistable area if  $\mathbf{k}_p = 0$  and  $\omega_p - \omega(\mathbf{k}_p) > 2\gamma$  and  $\gamma$  is independent of  $\mathbf{k}$ .

In the limit of small  $\gamma$  and large  $D = \omega_p - \omega(\mathbf{k}_p)$ , threshold  $P$  can be arbitrarily smaller than  $B_1 \gtrsim D/3$ . It is guaranteed near  $\mathbf{k}_p = 0$ , but, generally speaking, can also be valid in a wide region of  $\mathbf{k}_p$  and  $\omega_p$  where resonant scattering  $(\mathbf{k}_p, \mathbf{k}_p) \rightarrow (\mathbf{k}, 2\mathbf{k}_p - \mathbf{k})$  along the dispersion curve is permitted.<sup>30,34</sup> This brings up the question on the evolution scenario at  $f \gtrsim f(P)$ . Since the signal gain rate at the threshold is zero [ $\max_{\mathbf{k}} \Gamma(\mathbf{k}, P) = 0$ ], one can presume a “soft” onset of the scattering in such a way that steady-state amplitudes  $|\psi(\mathbf{k})|$  do not exhibit discontinuity near the threshold. This scenario is analogous to the second-order phase transition and, as such, is often opposed to a “rigid” development of instability at  $f = f(B_1)$  that involves jump in  $|\psi(\mathbf{k}_p)|$ .<sup>3,4,30,34,35</sup> In following Sec. III we prove that, although the increase of scattering “signals” can be arbitrarily slow and smooth in its beginning, even at constant  $f$  it is followed by a blowup, and finally the blueshift compensates the initial mismatch  $D$ .

### III. INEVITABILITY OF THE CATASTROPHE

#### A. Seeking for steady states

Above we have shown that on reaching the threshold the pumped mode starts to break up, giving rise to the growth of scattering “signals”. Now we seek for the conditions under which this process stops, resulting in a new steady-state field distribution.

Taking Eq. (2) at  $\mathbf{k} = \mathbf{k}_p$ , one finds that  $\psi_p \equiv \psi(\mathbf{k}_p)$  obeys the equation

$$\begin{aligned} i \frac{d}{dt} \psi_p(t) &= [\omega(\mathbf{k}_p) - i\gamma(\mathbf{k}_p)] \psi_p(t) + f(t) e^{-i\omega_p t} \\ &+ V |\psi_p(t)|^2 \psi_p(t) + 2V \psi_p(t) \sum_{\mathbf{k} \neq \mathbf{k}_p} \psi^*(\mathbf{k}, t) \psi(\mathbf{k}, t) \\ &+ V \psi_p^*(t) \sum_{\mathbf{k} \neq \mathbf{k}_p} \psi(2\mathbf{k}_p - \mathbf{k}, t) \psi(\mathbf{k}, t) \\ &+ V \sum_{\substack{\mathbf{q}_1 \neq \mathbf{k}_p, \mathbf{q}_2 \neq \mathbf{k}_p \\ \mathbf{q}_1 + \mathbf{q}_2 \neq 2\mathbf{k}_p}} \psi^*(\mathbf{q}_1 + \mathbf{q}_2 - \mathbf{k}_p, t) \psi(\mathbf{q}_1, t) \psi(\mathbf{q}_2, t). \end{aligned} \quad (12)$$

It is appropriate to neglect the last sum (that is independent of  $\psi_p$ ) on the assumption of a continuous  $k$ -space distribution of scattered modes so that  $|\psi(\mathbf{k})/\psi_p| \ll 1$  for each  $\mathbf{k} \neq \mathbf{k}_p$ ; note as well that related scattering processes can hardly obey the conservation laws (6). The remaining terms take account of all processes of the types  $(\mathbf{k}_p, \mathbf{k}) \leftrightarrow (\mathbf{k}, \mathbf{k}_p)$  and  $(\mathbf{k}_p, \mathbf{k}_p) \leftrightarrow (\mathbf{k}, 2\mathbf{k}_p - \mathbf{k})$ .

Let

$$\psi_p(t) = \tilde{\psi}_p e^{i\phi_0} e^{-i\omega_p t}, \quad \psi(\mathbf{k}, t) = \tilde{\psi}(\mathbf{k}) e^{i\phi(\mathbf{k})} e^{-i\tilde{\omega}(\mathbf{k})t}, \quad (13)$$

where all  $\tilde{\psi}$  take real and nonnegative values. Together with Eq. (6) it enables us to exclude high-frequency oscillations ( $\propto e^{-i\omega_p t}$ ) and transition effects and write the equation for  $\tilde{\psi}_0$  in the form of Eq. (3), i. e.

$$\tilde{\psi}_p^2 = \frac{f^2}{[\omega_p - \tilde{\omega} - V\tilde{\psi}_p^2]^2 + \tilde{\gamma}^2}, \quad (14)$$

where

$$\begin{aligned} \tilde{\omega} &= \omega(\mathbf{k}_p) + 2V \sum_{\mathbf{k} \neq \mathbf{k}_p} \tilde{\psi}^2(\mathbf{k}) \\ &+ V \sum_{\mathbf{k} \neq \mathbf{k}_p} \tilde{\psi}(\mathbf{k}) \tilde{\psi}(2\mathbf{k}_p - \mathbf{k}) \cos \chi(\mathbf{k}), \end{aligned} \quad (15)$$

$$\tilde{\gamma} = \gamma(\mathbf{k}_p) + V \sum_{\mathbf{k} \neq \mathbf{k}_p} \tilde{\psi}(\mathbf{k}) \tilde{\psi}(2\mathbf{k}_p - \mathbf{k}) \sin \chi(\mathbf{k}), \quad (16)$$

$$\chi(\mathbf{k}) = \phi(\mathbf{k}) + \phi(2\mathbf{k}_p - \mathbf{k}) - 2\phi_0. \quad (17)$$

Mean amplitude  $\tilde{\psi}_p$  depends on both the external field and the distribution of amplitudes  $\tilde{\psi}(\mathbf{k})$  and phases  $\chi(\mathbf{k})$  of scattered states. Values  $\tilde{\omega}$  and  $\tilde{\gamma}$  have the meaning of the frequency and decay rate of the driven mode. In particular,  $\tilde{\gamma} - \gamma(\mathbf{k}_p)$  represents its losses per unit time through the scattering from  $\mathbf{k} = \mathbf{k}_p$  to  $\mathbf{k} \neq \mathbf{k}_p$ . Thus, (i)  $\tilde{\gamma} - \gamma(\mathbf{k}_p) > 0$  as long as  $\sum_{\mathbf{k} \neq \mathbf{k}_p} \tilde{\psi}(\mathbf{k}) > 0$  and (ii)  $\sin \chi(\mathbf{k}) > 0$  as long as  $\tilde{\psi}(\mathbf{k}) > 0$ .

An equilibrium steady-state field distribution, if it exists, implies conservation of energy under constant pumping; in particular, balance of energy should be fulfilled between the driven mode and the set of scattered modes. It means that a virtual increase in  $\bar{\gamma}$ , that is connected with a virtual growth of non-zero “signals”, should involve a decrease in the steady-state amplitude of the driven mode that feeds them; hence,

$$\frac{\delta \bar{\psi}_p^2}{\delta \bar{\gamma}} < 0. \quad (18)$$

Indeed, the contrary would mean an increase in both the energy of intra-cavity field (as the interaction is repulsive and energy-conserving) and the energy lighting out of the cavity.

Now let us find the conditions under which an equilibrium can take place in the sense of Eq. (18). Taking the differential of Eq. (14), we have

$$\delta \bar{\psi}_p^2 = 2\bar{\psi}_p^2 \cdot \frac{\delta X}{Y}, \quad (19)$$

where

$$\delta X = (\omega_p - \bar{\omega} - V\bar{\psi}_p^2)\delta\bar{\omega} - \bar{\gamma}\delta\bar{\gamma}, \quad (20)$$

$$Y = (\omega_p - \bar{\omega} - V\bar{\psi}_p^2)^2 - 2V\bar{\psi}_p^2(\omega_p - \bar{\omega} - V\bar{\psi}_p^2) + \bar{\gamma}^2. \quad (21)$$

From Eq. (14) one sees that  $\partial(f^2)/\partial(\bar{\psi}_p^2) = Y$ . Accordingly,  $Y$  turns to zero at

$$\bar{\psi}_p^2 = \bar{B}_{1,2} \equiv \frac{2}{3}(\omega_p - \bar{\omega}) \mp \frac{1}{3}\sqrt{(\omega_p - \bar{\omega})^2 - 3\bar{\gamma}^2}. \quad (22)$$

$\bar{B}_1$  is the catastrophe point in which the steady-state amplitude exhibits discontinuity. Let us find the minimum of  $\delta X/\delta\bar{\gamma}$  at  $V\bar{\psi}_p^2 \leq \bar{B}_1$ . We have

$$\delta X \geq \frac{1}{3} \left( \omega_p - \bar{\omega} + \sqrt{(\omega_p - \bar{\omega})^2 - 3\bar{\gamma}^2} \right) \delta\bar{\omega} - \bar{\gamma}\delta\bar{\gamma}. \quad (23)$$

Then assume that  $\omega_p - \bar{\omega} > \sqrt{3}\bar{\gamma}$ ; consequently,

$$\frac{1}{\bar{\gamma}} \frac{\delta X}{\delta\bar{\gamma}} > \frac{1}{\sqrt{3}} \frac{\delta\bar{\omega}}{\delta\bar{\gamma}} - 1. \quad (24)$$

Estimate  $\delta\bar{\omega}/\delta\bar{\gamma}$  at  $\delta\bar{\gamma} > 0$ ,  $\delta\chi(\mathbf{k}) = 0$ , and  $\delta\bar{\psi}(\mathbf{k}) \geq 0$  for each  $\mathbf{k} \neq \mathbf{k}_p$ . It is appropriate to assume that

$$\sum_{\mathbf{k} \neq \mathbf{k}_p} \bar{\psi}(2\mathbf{k}_p - \mathbf{k})\delta\bar{\psi}(\mathbf{k}) \leq \sum_{\mathbf{k} \neq \mathbf{k}_p} \bar{\psi}(\mathbf{k})\delta\bar{\psi}(\mathbf{k}); \quad (25)$$

equality means equal gain rates of “signal” and “idler”. Then we have

$$\frac{\delta\bar{\omega}}{\delta\bar{\gamma}} \geq \frac{\sum_{\mathbf{k} \neq \mathbf{k}_p} u(\mathbf{k})\delta v(\mathbf{k})}{\sum_{\mathbf{k} \neq \mathbf{k}_p} \delta v(\mathbf{k})}, \quad (26)$$

where

$$u(\mathbf{k}) = \frac{2 + \cos\chi(\mathbf{k})}{\sin\chi(\mathbf{k})}, \quad \delta v(\mathbf{k}) = \sin\chi(\mathbf{k})\bar{\psi}(2\mathbf{k}_p - \mathbf{k})\delta\bar{\psi}(\mathbf{k}). \quad (27)$$

Note,  $\bar{\psi}(\mathbf{k}) > 0$  implies  $\sin\chi(\mathbf{k}) > 0$ . Hence, (26) is the average of  $u(\mathbf{k}) > 0$  over the region with  $\delta v(\mathbf{k}) > 0$  and, therefore,

$$\frac{\delta\bar{\omega}}{\delta\bar{\gamma}} \geq \min_{\chi} \left| \frac{2 + \cos\chi}{\sin\chi} \right| = \sqrt{3}; \quad (28)$$

the minimum is reached at  $\chi = 2\pi/3$ . Combining Eqs. (24) and (28), we finally have

$$\frac{\delta \bar{\psi}_p^2}{\delta \bar{\gamma}} > 0 \quad \text{everywhere at } P < V\bar{\psi}_p^2 < \bar{B}_1. \quad (29)$$

The result obtained proves that (i) slightly above the threshold the scattering involves growth of  $\bar{\psi}_p$ ; and that (ii) balance of energy between the pumped mode and scattered modes cannot be established below the catastrophe point.

## B. Stability analysis

Let us now analyze asymptotic stability of stationary solutions (14). Let

$$\psi_p(t) = \bar{\psi}_p e^{-i\omega_p t + i\phi_0} + \psi_1 e^{-i\Omega t} + \psi_2 e^{-i(2\omega_p - \Omega)t}. \quad (30)$$

Following the standard procedure, we substitute it into Eq. (12), take account of the steady-state equation for  $\bar{\psi}_p$  (so that corresponding terms disappear), and keep only the first powers of  $\psi_{1,2}$ . Equation of the type  $Qe^{-i\Omega t} + Re^{-i(2\omega_p - \Omega)t} = 0$  yields two separate equations  $Q = 0$  and  $R = 0$ . Then we have

$$\begin{pmatrix} A - \Omega & C \\ -C^* & 2\omega_p - A^* - \Omega \end{pmatrix} \begin{pmatrix} \psi_1 \\ \psi_2^* \end{pmatrix} = 0, \quad (31)$$

where

$$A = \omega_0 - i\gamma_0 + 2V(\bar{\psi}_p^2 + S_1), \quad (32)$$

$$C = V(\bar{\psi}_p^2 + \langle e^{i\chi} \rangle S_2) e^{2i\phi_0}, \quad (33)$$

where, in turn,  $\omega_0 = \omega(\mathbf{k}_p)$  and  $\gamma_0 = \gamma(\mathbf{k}_p)$  are the “unperturbed” quantities and

$$S_1 = \sum_{\mathbf{k} \neq \mathbf{k}_p} \bar{\psi}^2(\mathbf{k}), \quad S_2 = \sum_{\mathbf{k} \neq \mathbf{k}_p} \bar{\psi}(\mathbf{k})\bar{\psi}(2\mathbf{k}_p - \mathbf{k}), \quad (34)$$

$$\langle e^{i\chi} \rangle = \frac{1}{S_2} \sum_{\mathbf{k} \neq \mathbf{k}_p} \bar{\psi}(\mathbf{k})\bar{\psi}(2\mathbf{k}_p - \mathbf{k})e^{i\chi(\mathbf{k})}. \quad (35)$$

We solve the characteristic equation for  $\Omega$  and then solve equation  $\text{Im}\Omega = 0$  for  $V\bar{\psi}_p^2$ . The roots read

$$\begin{aligned} V\bar{\psi}_p^2 &= \bar{B}'_{1,2} \equiv \frac{2}{3}(\omega_p - \bar{\omega}) + S_2 \langle \cos\chi \rangle \\ &\mp \frac{1}{3} \sqrt{[\omega_p - \bar{\omega} + 3S_2 \langle \cos\chi \rangle]^2 + 3S_2^2 [1 - \langle \cos\chi \rangle^2] - 3\gamma_0^2}; \end{aligned} \quad (36)$$

interval  $\bar{B}'_1 < V\bar{\psi}_p < \bar{B}'_2$  is the forbidden zone where  $\text{Re}\Omega = \omega_p$  and  $\text{Im}\Omega > 0$ . In the above formula we have expressed  $S_1$  in terms of  $\omega_p - \bar{\omega}$ ,  $S_2$ , and  $\chi$  using Eq. (15).

Equation (36) shows that despite a decrease in  $\omega_p - \bar{\omega} - \bar{\gamma}$  the system is still bistable. It is not allowed to accumulate large energy in scattered modes while keeping  $\bar{\psi}_p$  relatively small. Normally,  $\bar{B}'_1 < \bar{B}_1$  unless  $S_2 \rightarrow 0$  and, hence,  $\bar{\gamma} \rightarrow \gamma_0$ .

Let us now estimate the total blueshift  $\bar{\omega} + V\bar{\psi}_p^2 - \omega_0$  above the instability area. Consider the ‘‘uncompensated’’ fraction of the pump detuning, i. e.

$$n = \frac{\omega_p - (\bar{\omega} + \bar{B}'_2)}{\omega_p - \omega_0} \quad (37)$$

at  $\gamma_0 \rightarrow 0$ . According to Eq. (36),  $n < 0$  at  $\langle \cos \chi \rangle > 0$ , but otherwise  $n$  can be positive. It reaches its maximum  $n_{\max} = 1/2$  at  $S_1 = S_2 = (\omega_p - \omega_0)/4V$  and  $\chi(\mathbf{k}) \rightarrow \pi$  for each  $\mathbf{k}$ , which, however, is impossible because it implies  $(\bar{\gamma} - \gamma_0)/(\bar{\omega} - \omega_0) \rightarrow 0$ . A more realistic case of  $\chi = 2\pi/3$  gives  $n_{\max} \approx 0.18$ . Thus, on the upper branch the total blueshift is close to or even exceeds the initial pump detuning.

We arrive at the conclusion that even at  $\omega_p - \omega_0 \gg \gamma_0$  an equilibrium cannot be reached until most of the pump frequency mismatch is compensated by the blueshift due to the increased field, irrespective of the system parameters.

### C. Dynamics of scattered modes

So far we have had no assumptions about  $\bar{\omega}$  and  $\bar{\gamma}$  those were just free parameters. However, we need to make a suggestion regarding the dependence of  $\bar{\gamma}$  on  $\bar{\psi}_p$  in view of the full system (2) rather than steady-state equation (14).

Let us consider the case of yet-uncompensated pump detuning, i. e.  $\omega_p - \bar{\omega} - V\bar{\psi}_p^2 \gg \gamma_0$ . The signal modes are distributed continuously and, thus,  $\bar{\psi}(\mathbf{k})/\bar{\psi}_p \ll 1$  for each  $\mathbf{k}$  but  $S_1$  can be comparable to  $\bar{\psi}_p^2$ . Therefore the Bogoliubov approximation [(7), (8)] is valid, allowing us to find renormalized eigenfrequencies  $\Omega$ . Let, for definiteness,  $\gamma(\mathbf{k}) = \gamma_0$  irrespective of  $\mathbf{k}$  and  $\mathbf{k}_p = 0$  so that  $S_1 = S_2 = S$ . Then we have

$$\Omega(\mathbf{k}) = \omega_p - i\gamma_0 \pm \sqrt{[\omega_p - \omega(\mathbf{k}) - 2V(S + \bar{\psi}_p^2)]^2 - V^2\bar{\psi}_p^4} \quad (38)$$

for  $\mathbf{k} \neq \mathbf{k}_p$ . Consider maximum gain rate  $\Gamma = \max_{\mathbf{k}} \text{Im}\Omega(\mathbf{k})$ . It is easy to see that  $\Gamma$  grows with  $V\bar{\psi}_p^2$  up to

$$V\bar{\psi}_p^2 \rightarrow Z \equiv \frac{2}{3}[\omega_p - \omega(\mathbf{k}_p) - 2S] = \frac{2}{3}(\omega_p - \bar{\omega}) + \frac{2}{3}S\langle \cos \chi \rangle > \bar{B}'_1. \quad (39)$$

Note as well that the unstable area is widening in the  $k$ -space up to  $V\bar{\psi}_p^2 = \bar{B}'_1$  [similar to Fig. 1(b)]. Hence, the worst-case ‘‘dynamical’’ assumption is that  $\bar{\gamma}$  grows with  $\bar{\psi}_p$  in the range of growing  $\Gamma$ , i. e.

$$\frac{d\bar{\gamma}}{d(\bar{\psi}_p^2)} > 0 \quad \text{at} \quad \bar{P} < V\bar{\psi}_p^2 \leq Z, \quad Z > \bar{B}'_1. \quad (40)$$

This allows us to bring together all results of this section.

### D. Hierarchy of instabilities and a route to the catastrophe

In the course of its evolution, the condensate passes through a chain of critical transformations.

The combination of Eqs. (29) and (40) means the positive feedback loop between  $\bar{\psi}_p$  and  $\bar{\gamma}$  which forms at  $V\bar{\psi}_p^2 = P$ . Since then both the pumped mode and scattering signals start to grow hyperbolically. However, at that early stage the pumped mode is still stable ‘‘by itself’’ in the sense that its growth is determined by the growth of signals, and the latter can be arbitrarily small in the vicinity of the threshold. This is the latency period whose duration is determined by  $f - f(P)$ .

Later, at  $V\bar{\psi}_p^2 = \bar{B}'_1$  [Eq. (36)] the system enters the strong positive feedback regime in which the driven mode could no longer keep its intensity fixed even at constant ‘‘signals’’. However, their gain rate still increases well above  $V\bar{\psi}_p^2 = \bar{B}'_1$  for each  $\langle e^{i\chi} \rangle$  according to Eq. (39). Consequently, at this stage the system cannot get stabilized at whatever phase and  $k$ -space distribution of scattered modes, and there is no way back.

Finally, at  $V\bar{\psi}_p^2 = \bar{B}_1$  [Eq. (22)] the feedback loop is short-circuited in the condensate mode, resulting in the explosive growth of its amplitude. Here the system drastically alters its state with respect to the external field and afterwards comes to the equilibrium.

## IV. MAIN RESULTS AND DISCUSSION

### A. Catastrophic behavior

The results of the previous section allow one to understand the dynamics of the condensate above the scattering threshold. Let us repeat the main points more informally.

The considered phenomena take place under above-resonance excitation. The break-up  $(\mathbf{k}_p, \mathbf{k}_p) \rightarrow (\mathbf{k}, 2\mathbf{k}_p - \mathbf{k})$  that begins at the threshold  $V\bar{\psi}_p^2 = P$  necessarily involves further growth of the pumped mode  $\bar{\psi}_p$ , even if the pump  $f^2$  remains constant. This is because approaching the resonance (due to the blueshift towards the pump frequency) compensates all additional losses brought on by strengthening the scattering from the pumped mode. As a result, its decay rate ( $\bar{\gamma}$ ) and frequency ( $\bar{\omega}$ ) increase continuously, and the distribution of scattered modes changes with time. It appears that modes with increasingly greater gain rates  $\Gamma$  successively get involved in scattering [see Fig. 1(b), (d)]. At the same time, the increase in either or both of  $\bar{\gamma}$  and  $\bar{\omega}$  lowers  $\bar{B}_1$ , the critical amplitude at which  $d\bar{\psi}_p/dt$  tends to infinity. The process of a ‘‘smooth’’ growth of  $\bar{\psi}_p$  cannot stop before meeting the catastrophe point  $V\bar{\psi}_p^2 = \bar{B}_1$ . Therein the field blows up. Finally equilibrium is reached when the initial mismatch  $\omega_p - \omega(\mathbf{k}_p)$  gets compensated by the polariton blueshift.

## B. OPO solutions

The final state of the system can be different depending on the pump wave vector  $\mathbf{k}_p$ . If  $\mathbf{k}_p = 0$ , all steady states are one-mode because the inter-mode scattering is impossible at  $V|\psi(\mathbf{k}_p=0)|^2 \geq B_2$  [see. Eq. (9)]. By contrast, if  $\mathbf{k}_p$  is near the inflection point of the polariton dispersion curve, then the final state can have macro-occupied ‘‘signal’’ ( $\mathbf{k}_s \approx 0$ ) and ‘‘idler’’ ( $\mathbf{k}_i \approx 2\mathbf{k}_p$ ) modes<sup>21,29</sup> whose average populations remain unchanged at a constant pump power, which is often referred to as polariton optical parametric oscillation (OPO).<sup>28,30</sup>

Regarding the OPO states, our findings shed light on one of their experimentally evidenced peculiarities. Namely, it is known that ‘‘signal’’ and ‘‘idler’’ appear at  $\mathbf{k}_s \approx 0$  and  $\mathbf{k}_i \approx 2\mathbf{k}_p$  irrespective of the pump detuning  $D = \omega_p - \omega(\mathbf{k}_p)$ ,<sup>29</sup> whereas the conservation laws (6) imply a broad ‘8’-shaped distribution of scattered modes as long as  $V\bar{\psi}_p^2 \gtrsim P$  and  $D > 0$ .<sup>3,21,35</sup> Such behavior can, however, easily be understood in view of the discussed scenario: the detuning  $D$  is compensated by the blueshift of the dispersion curve [Sec. III B], which yields  $\mathbf{k}_s \approx 0$  irrespective of  $D$ . In this respect our work supplements and explains the findings by D. Whittaker who showed that three-mode OPO states become asymptotically stable not earlier than the excitation density reaches a certain comparatively large magnitude.<sup>30</sup> Note as well that the hypothesis for the crucial role of the bistability in OPO formation was made already in Refs. 3 and 4. In the experimental work 21 employing cw pump conditions it was shown that a broad ‘8’-shaped distribution of scattered modes, that is observed in the linear regime, immediately turns into the three-mode OPO state on reaching the parametric threshold; in other words, reaching the threshold is accompanied by a jump in the polariton energy. At the same time, essentially collective phenomena were shown to play a role in OPO formation dynamics.<sup>20</sup> Finally, in this work we have found that it is general that reaching the parametric scattering threshold at  $D \gg \gamma$  involves sharp and very significant jump in energy, and that such effect is essentially collective.

## C. Accumulation of energy

Under a continuous-wave excitation the threshold of the transition between steady states coincides with the scattering threshold and, hence, is comparable to  $\gamma$  [see (10)]. At  $\mathbf{k}_p = 0$  the threshold pump density is

$$f_{\text{thr}}^2 = f^2(P) = \frac{\gamma}{V} [(D - \gamma)^2 + \gamma^2], \quad (41)$$

where  $D = \omega_p - \omega(\mathbf{k}_p)$ ; the existence of the high-energy solution at the same  $f$  is ensured by Eq. (11). Then integrally

$$V|\psi(\mathbf{k}_p)|^2 < \gamma \quad \text{if } f < f_{\text{thr}}, \quad (42)$$

$$V|\psi(\mathbf{k}_p)|^2 > D \quad \text{if } f > f_{\text{thr}}. \quad (43)$$

Note that Eq. (43) is also characteristic of a one-mode bistable oscillator (like that considered in Ref. 2), but in that case the

threshold  $f_{\text{thr}}^2 = f^2(B_1)$  does not depend on  $\gamma$  at  $\gamma/D \rightarrow 0$  and grows as  $D^3/V$  with increasing pump frequency. By contrast, we have shown that in a system with a high density of states the threshold can be infinitesimally small at  $\gamma \rightarrow 0$ ; and, assuming that the threshold is reached, the steady-state response is strong [ $V|\psi|^2 \gtrsim D$ ] in a very wide range of pump frequencies up to  $D = 3Vf^2/2\gamma^2$  [so that  $f^2 \geq f^2(B_2)$ ]. Thus, even under a weak pump the energy is gradually accumulated in the signal modes and with time becomes sufficient for the transition to the upper steady-state branch. Near the threshold,  $d\Gamma/df^2 \rightarrow V/D^2$  at  $\gamma \rightarrow 0$  [see Fig. 1(c) and Eq. (41)], so the time of energy accumulation can be large yet it does not tend to infinity at  $\gamma \rightarrow 0$  but is determined by the values of  $f - f_{\text{thr}}$  and  $D$ . Thus, it turns out that at  $f(P) \lesssim f < f(B_1)$  the pump intensity determines the latency period of the transition rather than the eventual field amplitude.

## V. NUMERICAL EXAMPLE

Below is an example of evolution of a resonantly pumped polariton system whose parameters correspond to Fig. 1 at above-threshold pump intensity  $f^2$  such that

$$f^2(P) : f^2 : f^2(B_1) \approx 1 : 1.1 : 3. \quad (44)$$

Equation (2) is solved on a square grid  $(k_x, k_y)$  of dimension  $81 \times 81$  and size  $-1.5 \leq k_{x,y} \leq 1.5 \mu\text{m}^{-1}$ . The pump wave vector  $\mathbf{k}_p = 0$ . To simulate scattering near the threshold, the right side of Eq. (2) is supplemented by a stochastic term  $\xi(\mathbf{k}, t)$  that has the properties of white noise:

$$\langle \xi(\mathbf{k}, t) \rangle = 0, \quad (45)$$

$$\langle \xi^*(\mathbf{k}_1, t_1) \xi(\mathbf{k}_2, t_2) \rangle = a\delta(\mathbf{k}_1, \mathbf{k}_2) \delta(t_1, t_2) \quad (46)$$

Its intensity  $a$  is sufficient for creating average background population  $V|\psi(\mathbf{k})|^2 \approx 10^{-9}P$  at  $f = 0$  for each  $\mathbf{k}$ , while its phase  $\arg \xi(\mathbf{k}, t)$  takes random values changing each 80 fs at each  $\mathbf{k}$ . Polariton lifetime  $\tau = 1/\gamma \approx 16$  ps; the full time interval on which Eq. (2) is solved lasts 1100 ps. The pump detuning and resonance width are  $\hbar[\omega_p - \omega(\mathbf{k}_p)] = 0.5$  meV and  $\hbar\gamma \approx 0.04$  meV, respectively.

Figure 2(a) presents the  $k$ -space and time distribution of the field,  $|\psi(k_x, t)|^2$  at  $k_y = 0$ . Figure 2(b) shows the intensities of the pump  $f^2$  and the driven mode  $|\psi(\mathbf{k}_p)|^2$  as functions of time, and Fig. 2(c) shows the integral intensity of scattered modes.

Pump intensity  $f^2$  increases linearly during 50 ps and then remains constant starting from  $t = 0$ . In the interval  $0 < t \lesssim 100$  ps, steadily correlated ‘‘signal’’ modes appear out of the noise substrate at  $k_x^2 + k_y^2 = |\mathbf{k}_s|^2$  [see also Fig. 1(b), (d)]. It is followed by the period of their exponential growth at a constant rate  $\Gamma \approx (1/3)\gamma(\mathbf{k}_s)$ . During this period ( $100 \lesssim t \lesssim 400$  ps) the signals are still weak and do not provide a significant feedback to the pumped mode, yet by  $t = 400$  ps a slight increase in  $|\psi(\mathbf{k}_p)|^2$  gets noticeable.

At  $t \approx 400$  ps the system reaches threshold  $V|\psi(\mathbf{k}_p)|^2 = \bar{B}'_1$  [Eq. (36)]. The renormalized dispersion surface now has a

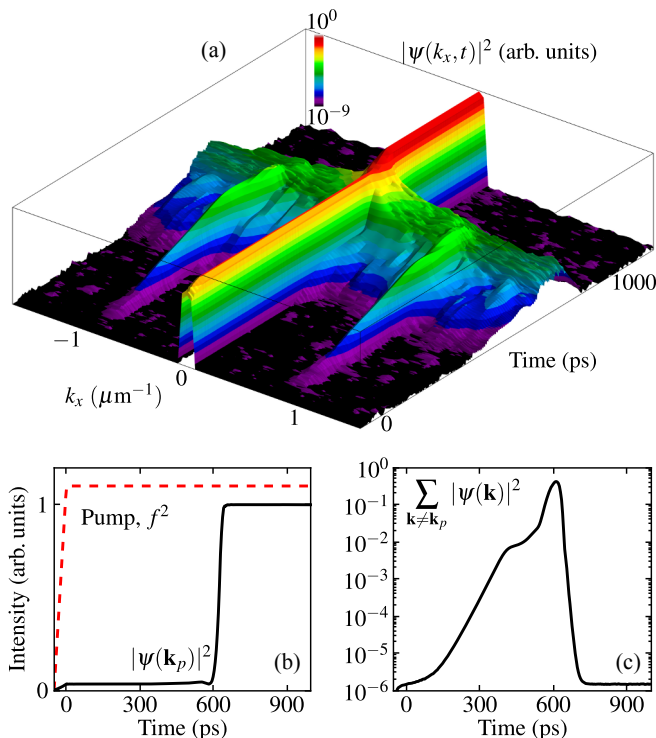


FIG. 2. (a) Distribution of intra-cavity field  $|\psi(k_x, t)|^2$  at  $k_y = 0$ ; (b) time dependences of  $f^2$  (dashed line) and  $|\psi(\mathbf{k}_p)|^2$  (solid line); (c) time dependence of  $\sum_{\mathbf{k} \neq \mathbf{k}_p} |\psi(\mathbf{k})|^2$ .

wide flat area  $[\tilde{\omega}(\mathbf{k}) = \omega_p]$  centered at  $\mathbf{k} = 0$ . Consequently, various scattering directions become permitted by the conservation laws. The scattering is “disordered”, the old signals go away from resonance but the new ones get out of the noise substrate and then grow quite rapidly. At  $t = 500$  ps,  $\sum_{\mathbf{k} \neq \mathbf{k}_p} |\psi(\mathbf{k})|^2$  is only one order of magnitude less than  $|\psi(\mathbf{k}_p)|^2$ , the latter being 30% larger than in the beginning of the process at  $t = 0$ .

Finally, in the catastrophe point the field grows explosively, and the system passes onto the upper steady-state branch ( $t = 600$  ps). Henceforth the scattering to  $\mathbf{k} \neq \mathbf{k}_p$  is no longer permitted by the conservation laws, so all the scattered modes reduce down to the noise level within the next 100 ps. The new one-mode state is stable and remains unchanged.

The scenario observed is general and reproduced irrespective of the number of nodes and size of the computational grid which, however, may strongly affect the characteristic evolution times. An important parameter is the noise amplitude  $\xi$  that in real systems is determined by quantum fluctuations and/or incoherent polariton states filled due to Rayleigh scattering on inhomogeneities. On one hand,  $a = \langle \xi^* \xi \rangle$  is the intensity level where the signal rises out of the noise; thus, the larger  $a$ , the smaller the time necessary for accumulating the critical energy in the course of a forthcoming regular increase at a given rate  $\Gamma$ . On the other hand, in the vicinity of  $f = f_{\text{thr}}$  fluctuations may cause a markable extension of a period when steadily correlated signal-idler pairs get out of the noise substrate. In our example it happens in the inter-

val  $0 < t \lesssim 100$  ps and then at  $400 \lesssim t \lesssim 500$  ps. To analyze fluctuations in a more tight connection to their physical origins, one should either simulate inhomogeneities and Rayleigh scattering<sup>18</sup> or use a probabilistic approach based on the Fokker-Planck equations<sup>36,37</sup> or take account of the exciton-phonon scattering and finite-temperature effects.<sup>38</sup>

## VI. CONCLUDING REMARKS

In this work we have found that coherently driven Bose condensates with a repulsive interaction can accumulate energy, which results in blowup-like dynamical scenarios. Above the threshold (41), the inter-particle interaction converts the difference between the driving wave ( $\omega_p$ ) and condensate ( $\omega_0$ ) frequency levels into the increased field  $|\psi|^2 \sim (\omega_p - \omega_0)/V$ , so that the blue-shift of the resonance compensates the mismatch of the pump frequency.

The discovered effect is expected to manifest itself in the transitions between steady states in multistable cavity-polariton systems. It should become pronounced in high- $Q$  microcavities with small decay rates  $\gamma$ . The smaller  $\gamma$ , the wider the range of pump frequencies  $\omega_p$  in which intra-cavity field grows with  $\omega_p$  at a given pump power and, at the same time, the lower the threshold density at a given  $\omega_p$ . However, there is a tradeoff between lowering the driving power and increasing the latency of the transitions. They still proceed at a comparatively weak pump but in that case they appear to be delayed in time with respect to the moment of reaching the threshold density [Fig. 2(b)].

Let us emphasize that the Gross-Pitaevskii equation is used on the assumption of a macroscopically coherent state of the field. Obviously, it cannot be true at whatever  $\omega_p - \omega_0$  in real finite-sized structures. However, it is definitely valid in GaAs based microcavities at  $(\omega_p - \omega_0)/\gamma \gtrsim 10$  and  $Q \gtrsim 10^4$  and pump spot sizes of about  $50 \mu\text{m}$ , which follows from a good agreement between modeled and measured data.<sup>16–18</sup> Note as well the possibility for the interaction strength  $V$  to depend on  $k_p$  and  $\omega_p$ . In cavity-polariton systems,  $V$  is determined by the exciton Hopfield coefficient, so it is of no use to pump the upper (photon-like) polariton branch far from resonance where  $V$  is nearly zero. Next, the discussed scenario will no longer make sense if the scattering threshold  $P$  gets greater than  $B_1$  [see Fig. 1(a)], which happens at large  $k_p$  beyond the “magic angle” [that is the inflection point in  $\omega_{\text{LP}}(k)$ , see Eq. (1)]. Finally, in this work we have neglected the spin degrees of freedom, assuming that all polaritons have just the same spin. Such assumption is appropriate as long as opposite-spin polaritons interact comparatively weakly, which, in its turn, normally appears to be the case<sup>39</sup> unless the pump frequency is very close to the exciton level<sup>19,40</sup> or TE/TM splitting gets noticeable at large  $k_p$  or a strong spatial anisotropy involves splitting of the orthogonally polarized eigenstates even at  $k = 0$ .<sup>16–18</sup>

The way of experimental verification of our findings is straightforward under both cw and pulsed excitation conditions. Under a cw excitation, one can track the dependence of the threshold pump density ( $f_{\text{thr}}^2$ ) on frequency detuning

$D = \omega_p - \omega(\mathbf{k}_p)$  at  $\mathbf{k}_p = 0$ . If our conclusions are correct,  $f_{\text{thr}}^2$  at  $D > 2\gamma$  should grow as  $\gamma D^2$  [Eq. (41)] instead of  $D^3$ ; the cubic dependence was predicted for the case of one-mode transitions.<sup>2</sup> On the other hand, the dynamics of the transitions between steady states can be observed directly with the use of pulsed excitation and time-resolved measurements on the scale of  $10^2$  ps. At comparatively small pump densities the system should reveal the latency period followed by a massive redistribution of scattered modes in the far field.

## ACKNOWLEDGEMENTS

I wish to thank V. D. Kulakovskii, N. A. Gippius, and S. G. Tikhodeev for stimulating discussions. 2D and 3D visualizations are performed using MATPLOTLIB<sup>41</sup> and MAYAVI,<sup>42</sup> respectively. I acknowledge financial support by the RF President grant No. MK-6521.2014.2 and the ‘‘Dy-nasty’’ foundation.

- 
- <sup>1</sup> V. F. Elesin and Y. V. Kopaev, *Sov. Phys. JETP* **36**, 767 (1973).  
<sup>2</sup> A. Baas, J. P. Karr, H. Eleuch, and E. Giacobino, *Phys. Rev. A* **69**, 023809 (2004).  
<sup>3</sup> N. A. Gippius, S. G. Tikhodeev, V. D. Kulakovskii, D. N. Krizhanovskii, and A. I. Tartakovskii, *EPL* **67**, 997 (2004).  
<sup>4</sup> N. A. Gippius and S. G. Tikhodeev, *Journal of Physics: Condensed Matter* **16**, S3653 (2004).  
<sup>5</sup> T. K. Paraíso, M. Wouters, Y. Léger, F. Morier-Genoud, and B. Deveaud-Plédran, *Nat Mater* **9**, 655 (2010).  
<sup>6</sup> D. Sarkar, S. S. Gavrilov, M. Sich, J. H. Quilter, R. A. Bradley, N. A. Gippius, K. Guda, V. D. Kulakovskii, M. S. Skolnick, and D. N. Krizhanovskii, *Phys. Rev. Lett.* **105**, 216402 (2010).  
<sup>7</sup> C. Adrados, A. Amo, T. C. H. Liew, R. Hivet, R. Houdré, E. Giacobino, A. V. Kavokin, and A. Bramati, *Phys. Rev. Lett.* **105**, 216403 (2010).  
<sup>8</sup> S. Gavrilov, A. Brichkin, A. Dorodnyi, S. Tikhodeev, N. Gippius, and V. Kulakovskii, *JETP Letters* **92**, 171 (2010).  
<sup>9</sup> S. S. Gavrilov, A. S. Brichkin, A. A. Demenev, A. A. Dorodnyy, S. I. Novikov, V. D. Kulakovskii, S. G. Tikhodeev, and N. A. Gippius, *Phys. Rev. B* **85**, 075319 (2012).  
<sup>10</sup> C. Weisbuch, M. Nishioka, A. Ishikawa, and Y. Arakawa, *Phys. Rev. Lett.* **69**, 3314 (1992).  
<sup>11</sup> Y. Yamamoto, T. Tassone, and H. Cao, *Semiconductor Cavity Quantum Electrodynamics* (Springer-Verlag, 2000).  
<sup>12</sup> A. V. Kavokin and G. Malpuech, *Cavity Polaritons* (Elsevier, Amsterdam, 2003).  
<sup>13</sup> N. A. Gippius, I. A. Shelykh, D. D. Solnyshkov, S. S. Gavrilov, Y. G. Rubo, A. V. Kavokin, S. G. Tikhodeev, and G. Malpuech, *Phys. Rev. Lett.* **98**, 236401 (2007).  
<sup>14</sup> I. A. Shelykh, T. C. H. Liew, and A. V. Kavokin, *Phys. Rev. Lett.* **100**, 116401 (2008).  
<sup>15</sup> S. S. Gavrilov, N. A. Gippius, S. G. Tikhodeev, and V. D. Kulakovskii, *JETP* **110**, 825 (2010).  
<sup>16</sup> S. S. Gavrilov, A. V. Sekretenko, S. I. Novikov, C. Schneider, S. Höfling, M. Kamp, A. Forchel, and V. D. Kulakovskii, *APL* **102**, 011104 (2013).  
<sup>17</sup> S. S. Gavrilov, A. V. Sekretenko, N. A. Gippius, C. Schneider, S. Höfling, M. Kamp, A. Forchel, and V. D. Kulakovskii, *Phys. Rev. B* **87**, 201303 (2013).  
<sup>18</sup> A. V. Sekretenko, S. S. Gavrilov, S. I. Novikov, V. D. Kulakovskii, S. Höfling, C. Schneider, M. Kamp, and A. Forchel, *Phys. Rev. B* **88**, 205302 (2013).  
<sup>19</sup> A. V. Sekretenko, S. S. Gavrilov, and V. D. Kulakovskii, *Phys. Rev. B* **88**, 195302 (2013).  
<sup>20</sup> A. A. Demenev, A. A. Shchekin, A. V. Larionov, S. S. Gavrilov, V. D. Kulakovskii, N. A. Gippius, and S. G. Tikhodeev, *Phys. Rev. Lett.* **101**, 136401 (2008).  
<sup>21</sup> D. N. Krizhanovskii, S. S. Gavrilov, A. P. D. Love, D. Sanvitto, N. A. Gippius, S. G. Tikhodeev, V. D. Kulakovskii, D. M. Whittaker, M. S. Skolnick, and J. S. Roberts, *Phys. Rev. B* **77**, 115336 (2008).  
<sup>22</sup> D. N. Krizhanovskii, E. A. Cerda-Méndez, S. S. Gavrilov, D. Sarkar, K. Guda, R. Bradley, P. V. Santos, R. Hey, K. Biermann, M. Sich, F. Frasn, and M. S. Skolnick, *Phys. Rev. B* **87**, 155423 (2013).  
<sup>23</sup> O. A. Egorov, D. V. Skryabin, A. V. Yulin, and F. Lederer, *Phys. Rev. Lett.* **102**, 153904 (2009).  
<sup>24</sup> O. A. Egorov, A. V. Gorbach, F. Lederer, and D. V. Skryabin, *Phys. Rev. Lett.* **105**, 073903 (2010).  
<sup>25</sup> M. Sich, F. Frasn, J. K. Chana, M. S. Skolnick, D. N. Krizhanovskii, A. V. Gorbach, R. Hartley, D. V. Skryabin, S. S. Gavrilov, E. A. Cerda-Méndez, K. Biermann, R. Hey, and P. V. Santos, *Phys. Rev. Lett.* **112**, 046403 (2014).  
<sup>26</sup> R. M. Stevenson, V. N. Astratov, M. S. Skolnick, D. M. Whittaker, M. Emam-Ismael, A. I. Tartakovskii, P. G. Savvidis, J. J. Baumberg, and J. S. Roberts, *Phys. Rev. Lett.* **85**, 3680 (2000).  
<sup>27</sup> C. Ciuti, P. Schwendimann, and A. Quattropani, *Phys. Rev. B* **63**, 041303 (2001).  
<sup>28</sup> D. M. Whittaker, *Phys. Rev. B* **63**, 193305 (2001).  
<sup>29</sup> R. Butté, M. S. Skolnick, D. M. Whittaker, D. Bajoni, and J. S. Roberts, *Phys. Rev. B* **68**, 115325 (2003).  
<sup>30</sup> D. M. Whittaker, *Phys. Rev. B* **71**, 115301 (2005).  
<sup>31</sup> D. W. McLaughlin, G. C. Papanicolaou, C. Sulem, and P. L. Sulem, *Phys. Rev. A* **34**, 1200 (1986).  
<sup>32</sup> M. J. Landman, G. C. Papanicolaou, C. Sulem, and P. L. Sulem, *Phys. Rev. A* **38**, 3837 (1988).  
<sup>33</sup> I. Carusotto and C. Ciuti, *Phys. Rev. Lett.* **93**, 166401 (2004).  
<sup>34</sup> M. Wouters and I. Carusotto, *Phys. Rev. B* **75**, 075332 (2007).  
<sup>35</sup> S. S. Gavrilov, N. A. Gippius, V. D. Kulakovskii, and S. G. Tikhodeev, *JETP* **104**, 715 (2007).  
<sup>36</sup> N. Maslova, R. Johne, and N. Gippius, *JETP Letters* **89**, 614 (2009).  
<sup>37</sup> R. Johne, N. S. Maslova, and N. A. Gippius, *Solid State Communications* **149**, 496 (2009).  
<sup>38</sup> Ö. Bozat, I. G. Savenko, and I. A. Shelykh, *Phys. Rev. B* **86**, 035413 (2012).  
<sup>39</sup> P. Renucci, T. Amand, X. Marie, P. Senellart, J. Bloch, B. Sermage, and K. V. Kavokin, *Phys. Rev. B* **72**, 075317 (2005).  
<sup>40</sup> M. Vladimirova, S. Cronenberger, D. Scalbert, K. V. Kavokin, A. Miard, A. Lemaître, J. Bloch, D. Solnyshkov, G. Malpuech, and A. V. Kavokin, *Phys. Rev. B* **82**, 075301 (2010).  
<sup>41</sup> J. D. Hunter, *Computing in Science and Engineering* **9**, 90 (2007).  
<sup>42</sup> P. Ramachandran and G. Varoquaux, *Computing in Science & Engineering* **13**, 40 (2011).